

# Experimental study of plate type air cooler performances under four operating modes

Yi Chen<sup>a</sup>, Hongxing Yang<sup>a,\*</sup>, Yimo Luo<sup>b</sup>

<sup>a</sup>*Renewable Energy Research Group (RERG), Department of Building Services Engineering,  
The Hong Kong Polytechnic University, Hong Kong*

<sup>b</sup>*Faculty of Science and Technology, Technological and Higher Education of Institute of Hong Kong, Hong Kong*

## Abstract

To reduce the chiller energy consumption in a central air-conditioning system, a heat exchanger, acting as an air cooler, can be installed before an air handling unit to pre-cool the fresh air by recovering cooling capacity from exhaust air. However, studies on evaluating the performances of air cooler under condensation condition are limited. Therefore, an experimental study was conducted to evaluate the plate type air cooler performance under four operating modes (dry/wet mode, low/high air humidity). Under dry operating mode, the air cooler serves as a traditional air cooler; while under wet operating mode, it works as an indirect evaporative cooler (IEC). The cooler dynamic performances during different operating mode transition were investigated. The steady performances under different parameter influence were also comparatively studied. The results show that wet operating improves the sensible and latent cooling capacities of air cooler significantly. Condensation takes place under high humidity inlet air, results in decreasing of sensible efficiency but increasing of latent efficiency and total heat transfer rate. The coefficient of performance (COP) of IEC is higher than that of traditional air cooler under the same testing configuration. The highest COP can reach 9.0 and achieved under wet operating mode with condensation.

---

\* Corresponding author. E-mail address: hong-xing.yang@polyu.edu.hk

**Keywords:** experiment, energy recovery, heat exchanger, indirect evaporative cooler, thermal performance

## **1. Introduction**

The air-conditioning system is well-known for intensive energy consumption, especially in hot regions where cooling is greatly needed [1,2]. It was reported that in Hong Kong the energy consumption for air conditioning in commercial buildings and residential buildings take up as much as 30% and 31% of the total building energy consumption, respectively [3]. To reduce the energy consumption in an air-conditioning system, energy recovery can be adopted by installing a heat exchanger before an air handling unit (AHU) to pre-cool the incoming fresh air using the exhaust air from air-conditioned space. The heat exchanger can be a traditional sensible air-to-air heat exchanger (plate, fin-plate and fin-tube), heat recovery wheel (sensible and enthalpy), indirect evaporative cooler (dry-coil and wet-coil) or any novel heat exchangers.

The traditional sensible air-to-air heat exchanger, acting as an air cooler, is regarded as a reliable and durable heat recovery device in a ventilated air-conditioning system, which is also introduced in ASHRAE Handbook [4]. The modeling of this device has been fundamentally studied. The simple model adopts uniform heat transfer coefficient and one-dimensional analysis [5]. The variations of heat transfer coefficient and air temperature along the fins were taken into consideration in some improved models [6,7]. A three-dimensional model for analyzing the performance of cross-flow fin-tube heat exchangers under dry and dehumidifying conditions was proposed by An and Choi [8]. The simulation results showed that for dehumidifying cases, the sensible heat transfer rate seemed insensitive to the inlet humidity change. Although the

modeling of such heat recovery device has been widely reported, limited experimental works had been presented in literatures. Fernandez-Seara et al. [9] experimentally analyzed an air-to-air heat recovery unit equipped with a sensible polymer plate heat exchanger (PHE) in residential buildings, but no condensation case was reported. Gendebien et al. [10] developed a model for an air-to-air heat exchanger dedicated to heat recovery ventilation considering dry (non-condensation) and partially wet regimes (condensation). The experimental tests were conducted but focused on validation of the proposed semi-empirical model.

Indirect evaporative cooler (IEC) is another heat exchanger which can be used for energy recovery in an air-conditioning system. It has been regarded as a promising energy-saving technology for its high efficient, low energy consumption, pollution-free and easy maintenance features [11,12]. Unlike the traditional heat exchanger, the IEC needs to be operated under wet condition and produces cooling air by water evaporation. The most commonly used plate-type IEC consists of a traditional plate-type heat exchanger, a water circulation and a distribution system. The heat exchanger is composed of alternative wet and dry channels which are separated by thin plates. In the wet channels, the spraying water drops form a thin water film on the plate surface and consistently evaporates into the main stream of the secondary air. The primary air in the adjacent dry channels is cooled by the low separating wall [13].

The IEC is widely used for cooling in hot and dry regions because larger cooling capacity can be achieved with low humidity fresh air [14~18]. The cooled primary air is supplied to the interior directly in these regions. In hot and humid regions, the supplied primary air temperature is limited to the high wet-bulb temperature of ambient air, so it is used as an energy recovery

device installed before an AHU or cooling coil in an air-conditioning system [19]. The exhausted air with lower wet-bulb temperature from air-conditioned space is used as secondary air to pre-cool the primary air (fresh air). This hybrid cooling system consisted of IEC and mechanical cooling receives great attention in recent years for its high energy saving potential [20~22].

The heat and mass transfer process of IEC has been fundamentally studied by analytical models and numerical models considering different factors, such as evaporation water loss, water film temperature variation, heat conduction of wall, variable Lewis factor and condensation from primary air [23~28]. The experimental study and field measurement have also been conducted to various kinds of IEC, aiming at: 1. testing the operational characteristics under the controlled laboratory and real building conditions; 2. verifying the established models. Tulsidasani et al. [29] experimentally tested the COP for a tube type IEC at India summer operation condition. It was found that the maximum COP reached 22. Qiu [30] tested a small scale IEC prototype and the poor wetting of plate surface was suspected from the results. Velasco Gómez [31] investigated a polycarbonate-made IEC under two operational modes: with spray water and without spray water. Experimental results proved the spraying water could enhance the cooling performance. Except the traditional tube type and plate type IEC, some novel IEC, such as two stage direct/indirect system, Regenerative IEC (RIEC), M-cycle, desiccant/IEC system with higher efficiency had also been tested and investigated. Jain [32] developed a two-stage evaporative cooler in order to enhance the effectiveness of IEC under high humidity condition. Kulkarni and Rajput [33] tested the performance of a two stage IEC and optimized the system by using different shapes and cooling media in the direct stage. Similar two-stage system had been tested by El-Dessouky et al. [34], Heidarinejad G et al. [35] and Jain [36]. Recently, Duan et al. [37] experimentally

investigated the operational performance (EER, wet-bulb efficiency, cooling capacity) and impact factors of a counter-flow RIEC. Cross flow and counter flow M-cycle IEC have also been experimentally tested for parameter study, optimization of geometry and operating conditions [38~41]. However, all the experimental work focuses on evaluating the sensible cooling ability of IEC. No experimental study can be found on evaluating both the sensible and latent cooling performance of IEC with condensation from primary air. It can be a research gap for IEC energy recovery technology applied in humid regions.

In sum, the intensive experimental study on evaluating the performances of both traditional air cooler and IEC with condensation is lacking. Under the high humidity condition, the primary air is not only sensibly cooled but also dehumidified. The simultaneous sensible and latent heat transfer process on the primary air side would make the cooling performance different from that of traditional dry cases. However, to the authors' best knowledge, the detailed sensible and latent cooling performances of the two kinds of air coolers have not been experimentally investigated.

To build the research gap, an experimental study was conducted to evaluate the plate type air cooler performance under four operating modes, including dry operating mode with low humidity air, dry operating mode with high humidity air, wet operating mode with low humidity air and wet operating mode with high humidity air. Under dry operating mode, the air cooler serves as a traditional air cooler; while under wet operating mode, it works as an IEC. So comparisons can be made between traditional air cooler and IEC under either non-condensation or condensation conditions. The cooler dynamic performances during different operating mode transition and steady performances under different parameter influence were investigated as well.

Nomenclature			
$c_{pa}$	specific heat of air, J/kg·°C	$Q$	heat transfer rate, W
$h_{fg}$	latent heat of vaporization of water, J/kg	$s$	channel gap, m
$i$	enthalpy of air, J/kg	$t$	Celsius temperature, °C
$m$	air mass flow rate, kg/s	$u$	air velocity, m/s
$P$	power consumption, W		
Greek symbols			
$\omega$	moisture content of air, g/kg	$\eta$	sensible efficiency
Subscripts			
$p$	primary/fresh air	$wb$	wet-bulb
$s$	secondary/exhaust air	$sen$	sensible heat
$out$	outlet air	$lat$	latent heat
$in$	inlet air	$tot$	total heat

## 2. Description of test rig

The schematic diagram and photograph of the test rig are shown in Fig.1 and Fig.2, respectively. A cross-flow plate type heat exchanger was designed and fabricated as the core component of the test rig. The heat exchanger is stacked with alternative primary air and secondary air channels which is separated by the thin aluminum plates. Both the channels are supported by the plastic corrugated sheets and the aluminum plates are hydrophilic-coated to improve its wettability. The geometric parameters of the experimental heat exchanger module are listed in Table 1. This heat exchanger can be used as a traditional air cooler, which uses the cool exhausted air from air-conditioned room to pre-cool the hot fresh air in an air-conditioning system for energy conservation.

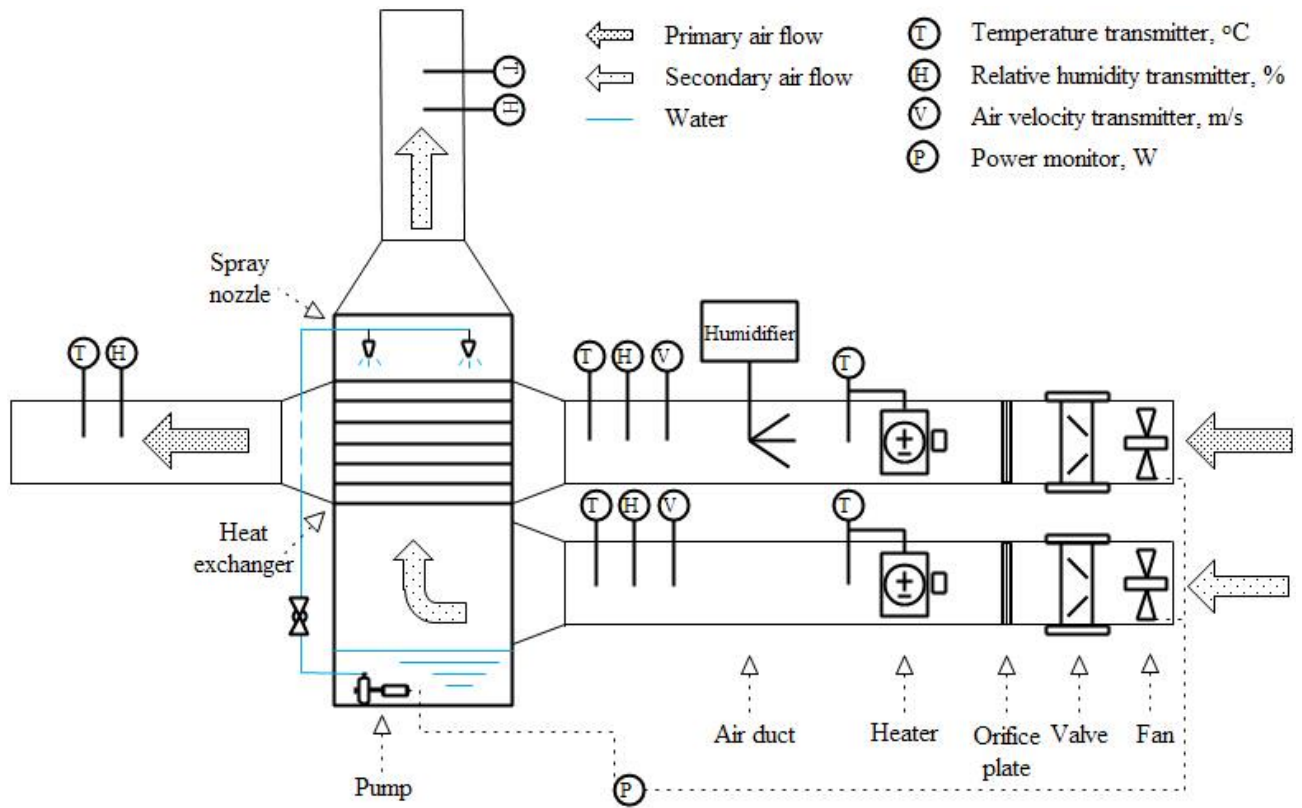


Fig.1 Schematic diagram of the test rig

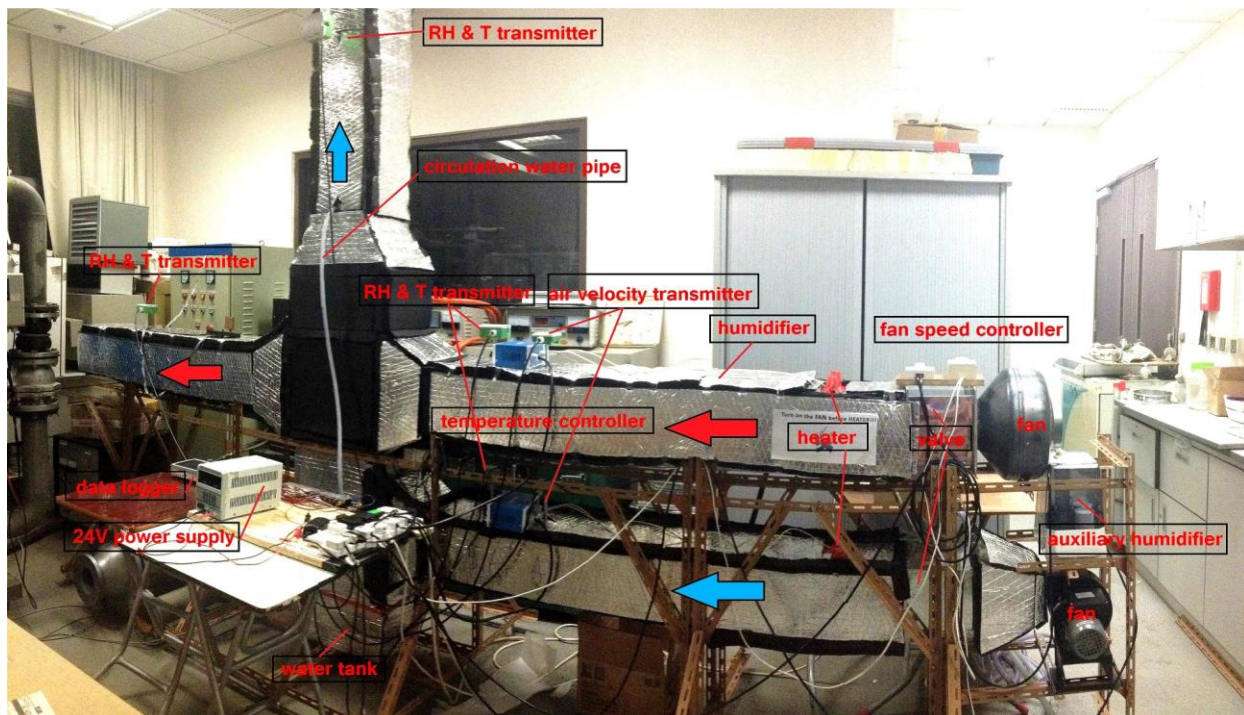


Fig.2 Real picture of the test rig

Table 1 Geometric parameters of experimental heat exchanger module

Parameters	Value
Cooler length ( $L$ )	0.4m
Cooler width ( $W$ )	0.2m
Cooler height ( $H$ )	0.4m
Primary air channel gap ( $s$ )	4mm
Secondary air channel gap ( $s$ )	4mm
Channel pairs ( $n$ )	25
Plate thickness ( $\delta$ )	0.15mm

An indirect evaporative cooler consisted of the above heat exchanger, a water circulation and distribution system has been assembled. Two water spray nozzles connected with the PVC pipes are hang vertically on the top of the heat exchanger to wet the secondary air channels. The pipes are supported by the steel angles inside the air duct. An submerged pump is fixed at the bottom of the water tank to enable the water spraying and circulation. The working principle of IEC for energy recovery is as follows. The exhausted air from the air-conditioned space would be attracted into the wet channels to work as secondary air from the bottom of heat exchanger by the fan. In the wet channels, the spraying water drops form a thin water film on the plate surface and consistently evaporates into the secondary air stream by absorbing heat from surroundings. The humidified secondary air is finally exhausted from the top of the heat exchanger. The primary air in the adjacent dry channels is cooled due to the temperature difference with the seperating wall. The primary air, which is the supplied fresh air in an air-conditioning system,



would be sensibly cooled without moisture change when the inlet primary air is dry, otherwise, it would be dehumidified with condensation when the inlet primary air is humid.

In sum, the plate type air cooler in the test rig can operate as two different air coolers. It works as an IEC when water spraying system is turned on and operates as a traditional air cooler without water spraying. To investigate and compare the cooling performance of the two kinds of air coolers under various operating conditions, an experimental setup was established. The test rig is composed of IEC, four air ducts (primary air inlet, primary air outlet, secondary air inlet and secondary air outlet), fans, valves, orifice plate, electrical heater, electrode humidifier, control devices and data collection system. The test rig is set up in a closed air-conditioned room, where the room temperature is controllable. The indoor air is used as both inlet primary air and secondary air, and then further treated by the heater and humidifier installed inside the ducts to reach a desired inlet air condition. The heat exchanger as well as all the air duct surfaces are insulated with neoprene foam to prevent heat loss to surroundings.

During the experiment, the air temperature can be adjusted to the pre-setting values by Proportion Integration Differentiation (PID) controllers. The variable speed controller is used to adjust the inlet air velocity entering the heat exchanger. The ranges of the controllable parameters in the experiment are summarized in Table 2. The primary air temperature is based on the temperature range in hot seasons, when the air-conditioning is needed. The secondary air conditions are based on the temperature and humidity ranges in an air-conditioned room. The humidification rate provided by the humidifier remains at a relative constant value when it operated. The data measuring devices included four temperature and humidity transmitters (Pt

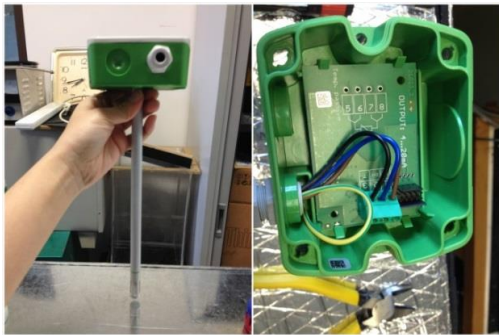
1000 sensor, E+E Co., Model: EE160), two air velocity transmitters (hot-film anemometer, E+E Co., Model: EE65) and one power meter. A 24V DC battery was used to provide the power supply to all the transmitters. The measurement instruments and specification are shown in Table 3. The photographs of measuring and control devices are shown in Fig.3.

Table 2 Summary of the ranges of various parameters

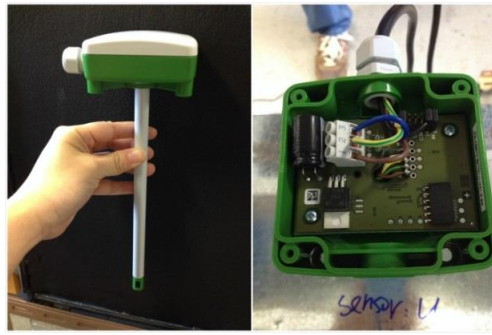
Parameter	Symbol	Unit	Range
Inlet primary air temperature	$t_{p,in}$	°C	27.1~34.4
Inlet primary air humidity	$\omega_{p,in}$	g/kg	12.1~20.5
Inlet primary air velocity	$u_{p,in}$	m/s	1.34~5.21
Inlet secondary air temperature	$t_{s,in}$	°C	22.3~28.4
Inlet secondary air humidity	$\omega_{s,in}$	g/kg	10.2~14.8
Inlet secondary air velocity	$u_{s,in}$	m/s	1.77~4.87

Table 3 Specification of different measuring instruments

Parameters	Device	Range	Accuracy
Air dry bulb temperature	Pt1000 Model: EE160	-15~60°C	±0.3°C
Air relative humidity	Pt1000 Model: EE160	10~95% RH	±2.5% RH
Air velocity	Hot film anemometer Model: EE65	0~10 m/s	±0.2m/s
Power consumption	Power meter	0~10A 0~2200W	0.01W



(a) RH & T transmitter



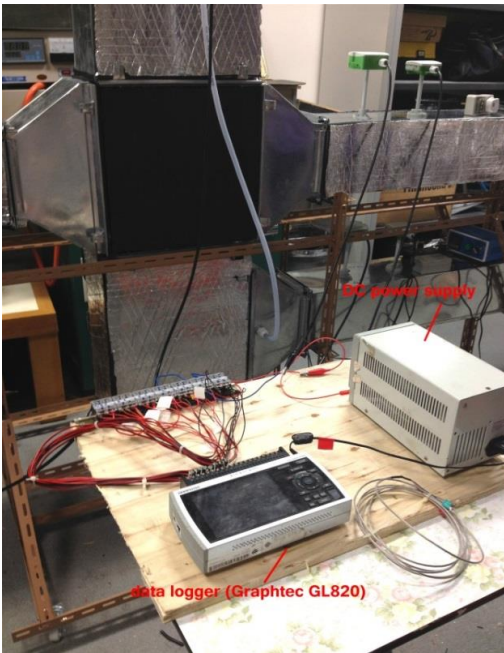
(b) Velocity transmitter



(c) Temperature PID controller



(d) Fan speed controller



(e) Data logger



(f) Power meter

Fig.3 Measuring and control device in the test rig

Under each test case, the inlet and outlet air parameters are measured by the transmitters and recorded by the data logger (GRAPHTEC GL820). The collected data include the inlet and outlet temperatures and relative humidity of primary air and secondary air, and inlet air velocities of the two air streams. All the air parameters data were recorded at 2 seconds step. The steady state is defined as the outlet temperature and relative humidity variations are within 0.1°C and 1% for 5 minutes. The average values of the measured data in the 5 minutes span are used for steady operation analysis. The power consumptions of the two air fans and circulation pump are measured by the power meter.

### **3. Four operating modes of air cooler**

Four operating modes of the air cooler are explored for comparison study, including: dry operation state with low humidity air, dry operation state with high humidity air, wet operation with low humidity air and wet operation with high humidity air. The on/off state of circulation pump distinguishes the wet and dry operating mode; and on/off state of humidifier creates the high and low humidity primary air. Under wet operating mode, the air cooler acts as an indirect evaporative cooler, while under dry operating mode, it is a traditional plate type air cooler. So the performances of the two kinds of air cooler can be compared under the same configuration. Meanwhile, the air cooler performance under high and low air humidity can also be experimentally investigated in order to compare the energy recovery performance in different climate regions. Under the low humidity primary air condition, there would be only sensible heat transfer on the primary air side. Under the high humidity primary air condition, however, the condensation is likely to take place in the primary air channels because the plate surface

temperature could be lower than the primary air dew point temperature. The schematic diagram of the heat and mass transfer process under the four operating modes is shown as Fig.4.

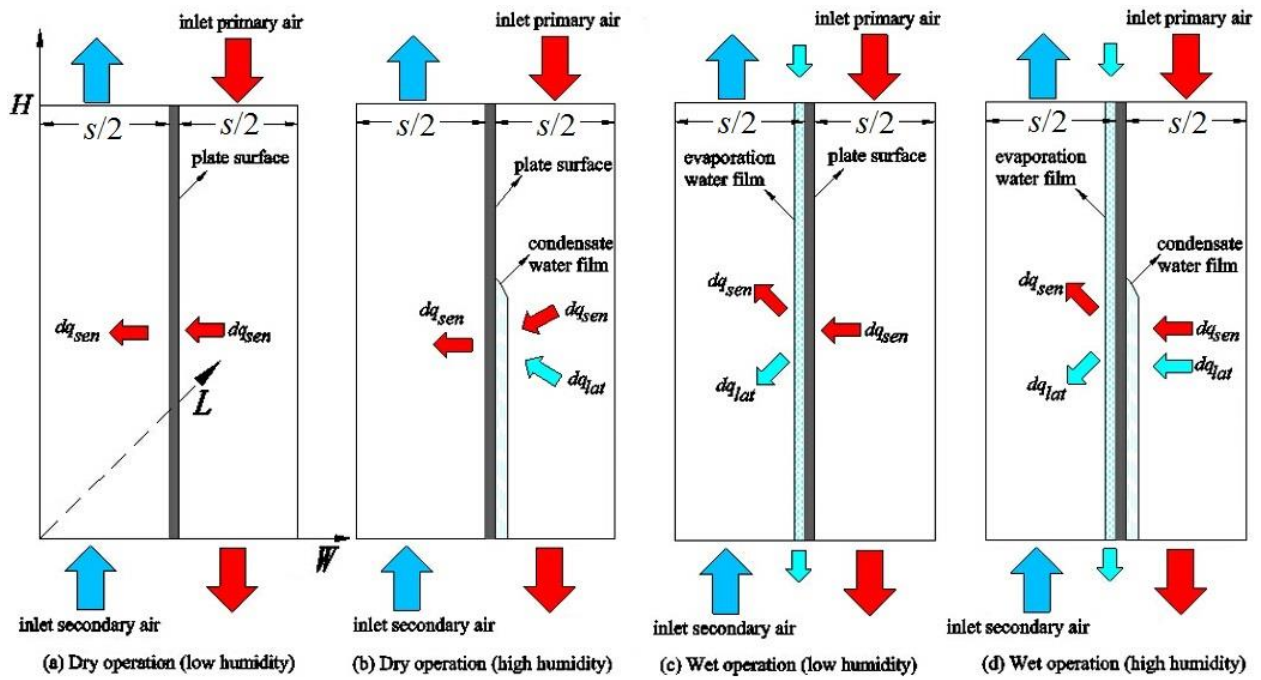


Fig.4 Heat and mass transfer process of heat exchanger under four operating modes

The settings of pump and humidifier, controllable parameters and performance indicators under four operating modes are listed in Table 4.

Table 4 Four operation modes in the experiment

Operation mode	HE Type	Circulation pump	Humidifier	Controllable parameters	Performance indicator
Dry operation (low humidity)	Traditional	Off	Off	$t_{p,in}, t_{s,in}$	$Q_{sen}, \eta, COP$
Dry operation (high humidity)	Traditional	Off	On	$u_{p,in}, u_{s,in}$	$Q_{sen}, Q_{lat}, Q_{tot}, \eta, \eta_{lat}, COP$

Wet operation (low humidity)	IEC	On	Off	$Q_{sen,}, \eta_{wb}, COP$
Wet operation (high humidity)	IEC	On	On	$Q_{sen,}, Q_{lat}, Q_{tot},$ $\eta_{wb}, \eta_{lat,}, COP$

#### 4. Performance indicator and uncertainty analysis

Sensible efficiency  $\eta$  is used to evaluate the sensible heat transfer of traditional heat exchanger, expressed as:

$$\eta = \frac{t_{p,in} - t_{p,out}}{t_{p,in} - t_{s,in}} \quad (1)$$

The wet-bulb effectiveness  $\eta_{wb}$  is usually used as an evaluation metric for rating an IEC, expressed as:

$$\eta_{wb} = \frac{t_{p,in} - t_{p,out}}{t_{p,in} - t_{wb,s,in}} \quad (2)$$

The above two performance indicators are commonly used for rating the traditional heat exchanger and IEC under non-condensation state, respectively. Under condensation state, latent efficiency  $\eta_{lat}$  is introduced for rating the latent heat transfer for both kinds of heat exchangers, given as:

$$\eta_{lat} = \frac{\omega_{p,in} - \omega_{p,out}}{\omega_{p,in} - \omega_{s,in}} \quad (3)$$

In this study, the traditional heat exchanger and IEC is used as energy recovery device or fresh air pre-cooling device in an air-conditioning system, thus their cooling capacity can be evaluated by the primary air cooling rate. The sensible cooling capacity, latent cooling capacity and total cooling capacity can be calculated as following equations, respectively.

$$Q_{sen} = m_p \cdot c_{pa} \cdot (t_{p,in} - t_{p,out}) \quad (4)$$

$$Q_{lat} = m_p \cdot h_{fg} \cdot (\omega_{p,in} - \omega_{p,out}) \quad (5)$$

$$Q_{tot} = Q_{sen} + Q_{lat} = m_p \cdot (i_{p,in} - i_{p,out}) \quad (6)$$

The coefficient of performance (COP) of an air cooler is defined as the ratio of total cooling capacity to total power consumption, expressed as:

$$COP = \frac{Q_{tot}}{P} = \frac{m_p \cdot (i_{p,in} - i_{p,out})}{P} \quad (7)$$

For the traditional heat exchanger, the total power consumption is contributed by the fans, while for IEC, the total consumption includes fans and pump.

The uncertainties of experimental results are caused by errors in the measuring process. The uncertainty analysis is conducted to examine the validity of collected data by measuring devices. The uncertainty analysis of all the measuring data in the experiment as well as the calculated performance indicators have been conducted using the method given in the reference [42]. The uncertainty analysis results are listed in Table 5.

Table 5 Uncertainty analysis results

Indicator	Nominal value	Relative uncertainty
-----------	---------------	----------------------

Symbol	Low humidity*	High humidity**	Low humidity*	High humidity**
$V_p$	288 m <sup>3</sup> /h	288 m <sup>3</sup> /h	± 4.5%	± 4.5%
$V_s$	360 m <sup>3</sup> /h	360 m <sup>3</sup> /h	± 3.6%	± 3.6%
$\eta$	45%	45%	± 8.7%	± 8.7%
$\eta_{wb}$	61%	51%	± 4.2%	± 4.8%
$\eta_{lat}$	0% (wet)	36% (wet)	NA	± 12.1%
	0% (dry)	0% (dry)	NA	NA
$Q_{sen}$	657 W (wet)	548 W (wet)	± 6.1 % (wet)	± 6.6% (wet)
	314 W (dry)	314 W (dry)	± 9.4 % (dry)	± 9.4% (dry)
$Q_{lat}$	0 W (wet)	718 W (wet)	NA (wet)	± 12.7% (wet)
	0 W (dry)	0 W (dry)	NA (dry)	NA (dry)
$Q_{tot}$	657 W (wet)	1266 W (wet)	± 6.1% (wet)	± 7.7% (wet)
	314 W (dry)	314 W (dry)	± 9.4% (dry)	± 9.4% (dry)
COP	5.2 (wet)	10.0 (wet)	± 6.1% (wet)	± 7.8% (wet)
	3.0 (dry)	3.0 (dry)	± 9.4% (dry)	± 9.4% (dry)

\* Low humidity:  $u_p=2.0$  m/s,  $u_s=2.5$  m/s,  $t_p=30$  °C,  $RH_p=45\%$ ,  $t_p=22.5$  °C,  $RH_s=68\%$ .

\*\*High humidity:  $u_p=2.0$  m/s,  $u_s=2.5$  m/s,  $t_p=30$  °C,  $RH_p=75\%$ ,  $t_p=22.5$  °C,  $RH_s=68\%$ .

## 5. Results and discussion

To ensure the reliability of the experiment results, the energy balance of the test rig is checked.

The experiment results are then presented from two aspects: 1. dynamic performance of air



cooler during operating mode transition; 2. steady performance of air cooler under different parameter influence.

### 5.1 Energy conservation analysis and results comparison with simulation

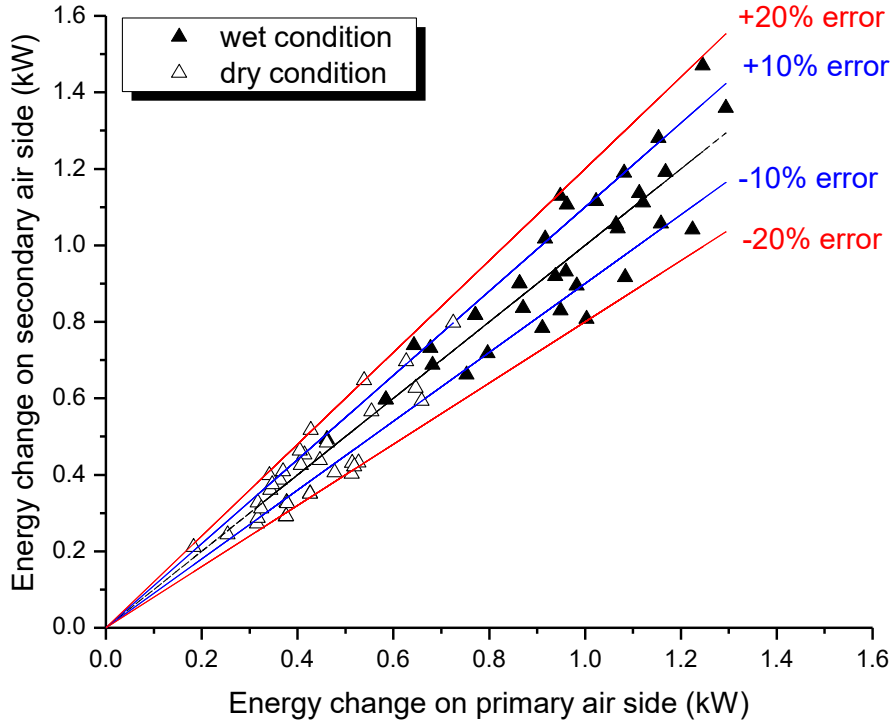


Fig.5 Energy balance of two air streams

The enthalpy reduction of primary air should be equal to the enthalpy increase of secondary air based on energy balance theory. The energy conservation equations on primary air side and secondary air side are given as:

$$Q_p = m_p \cdot (i_{p,in} - i_{p,out}) \quad (8)$$

$$Q_s = m_s \cdot (i_{s,out} - i_{s,in}) \quad (9)$$

Fig.5 presents the comparison of enthalpy changes between the two air streams under both wet and dry operating conditions. The discrepancies of all the experiment results are found to be within  $\pm 20\%$ .

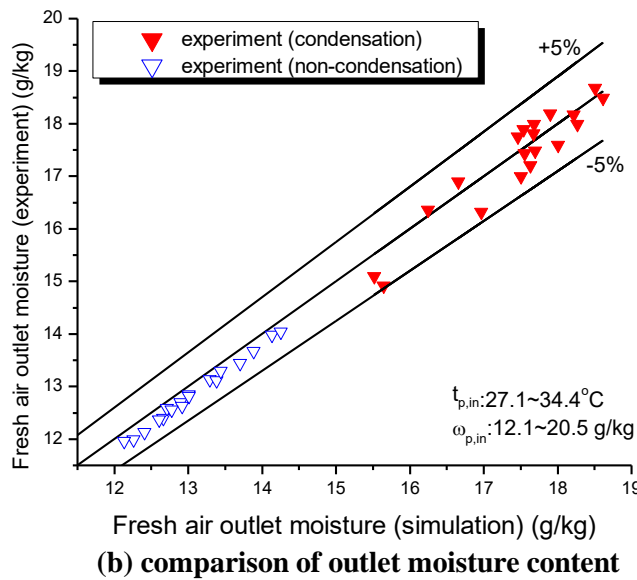
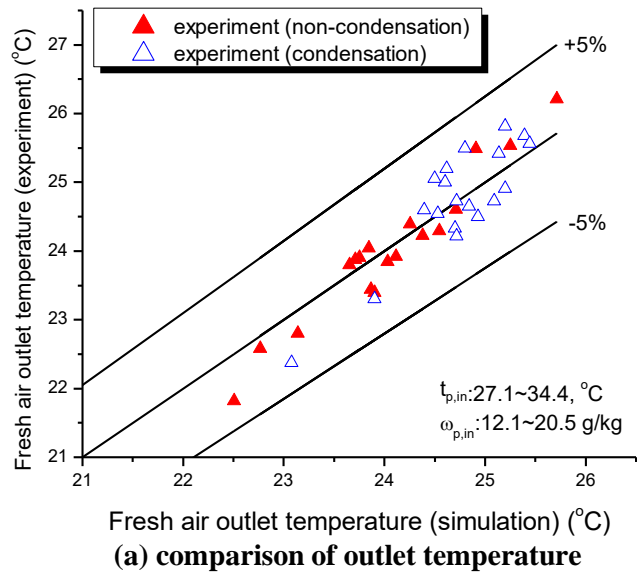


Fig.6 Comparison of primary air outlet conditions between experiment and simulation

All the experiment results under wet operating mode (IEC mode) are compared with the simulation results by setting the same operating conditions and unit configuration, as shown in

Fig.6. The simulation was conducted by the numerical model published in previous paper [43]. It is found that discrepancies in predicting IEC outlet temperature and humidity are within  $\pm 5\%$  under both condensation and non-condensation states.

## **5.2 Dynamic performance when switching operating mode**

Dynamic performance of the air cooler when switching from one operating mode to another is experimentally studied. The air parameters were monitored from the initial steady operating state to the variation process when one operation condition changed (turn on the pump or humidifier), and finally to another steady operating state. The influence of certain operating condition could be observed clearly through the dynamic test. Four representative cases were tested. The simulation results of the outlet parameters [43] under the final steady conditions are plotted (marked by a straight line) in all the figures in order to be compared with experiment results.

### **5.2.1 Switch from dry to wet operating mode (low humidity primary air)**

Fig.7 shows the temperature variation of outlet primary air when the air cooler is switched from dry to wet operating mode under low humidity inlet air condition. It can be seen that the outlet primary air temperature decreases as soon as the circulation pump is turned on and the air cooler is changed from a traditional air cooler to an IEC. The temperature decreases dramatically from the initial steady state of  $29.5^{\circ}\text{C}$  to another steady state of  $26.6^{\circ}\text{C}$ .

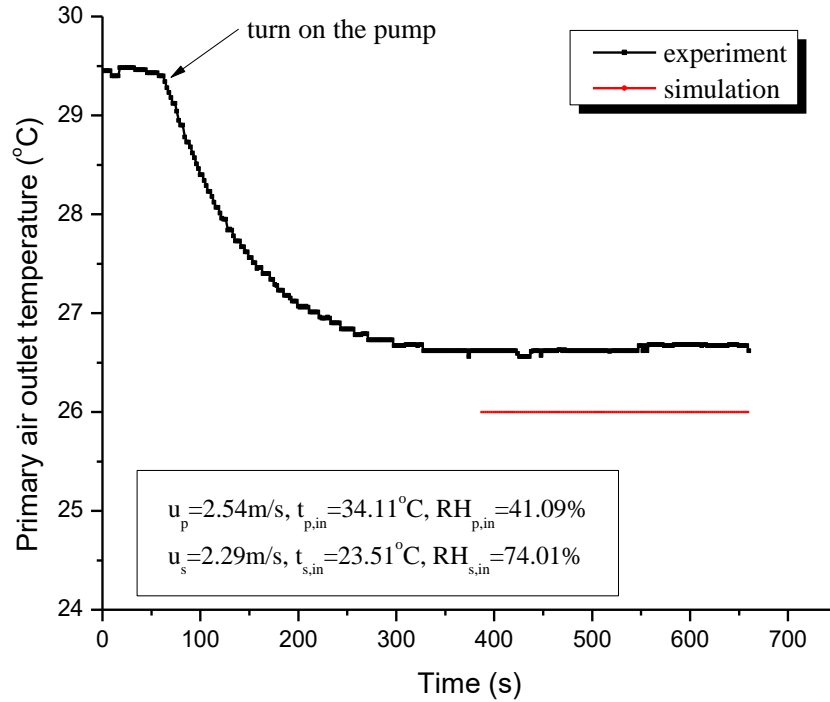
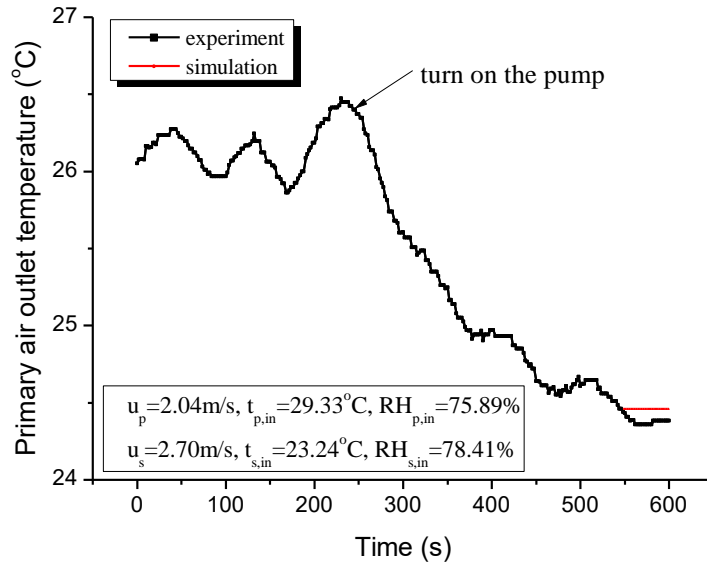


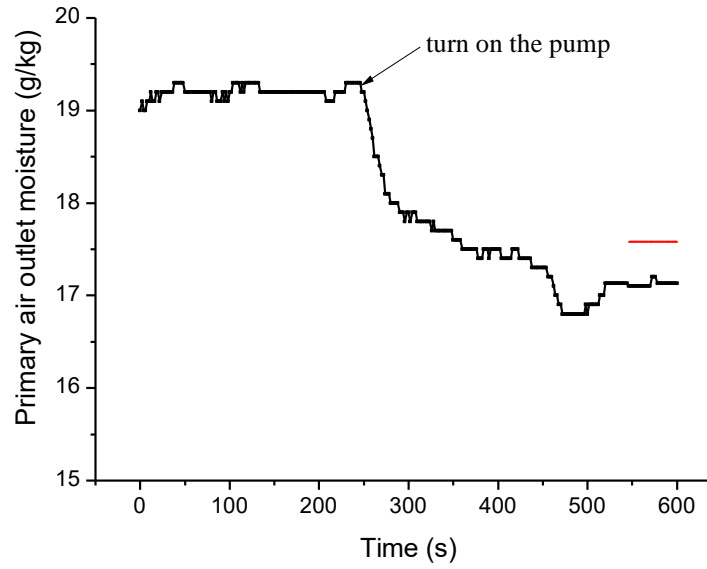
Fig.7 Outlet air temperature variation when switching from dry to wet operating mode (low humidity primary air)

The decrease of outlet air temperature indicates the increase of cooling capacity and enhancement of heat transfer process. The improvement of cooling capacity under wet operating mode is because the water film in the secondary air channels lowers the plate surface temperature and improves the heat transfer rate by evaporation. It can be calculated that the total heat transfer rate under dry operating mode in Fig.7 is 541 kW, while it is 882 kW under wet operating mode, 63% larger than that of dry operating mode. So the cooling capacity of IEC is greatly improved compared with that of traditional air cooler.

5.2.2 Switch from dry to wet operating mode (high humidity primary air)



(a) outlet primary air temperature



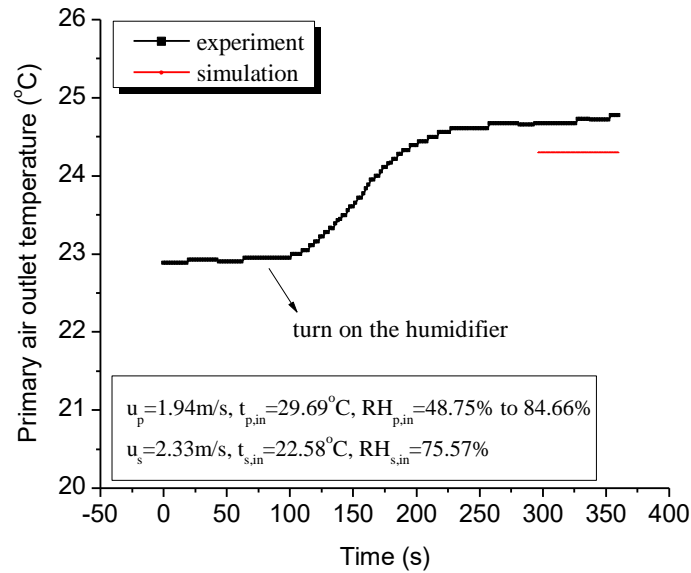
(b) outlet primary air moisture content

Fig.8 Outlet air temperature and humidity variation when switching from dry to wet operating mode (high humidity primary air)

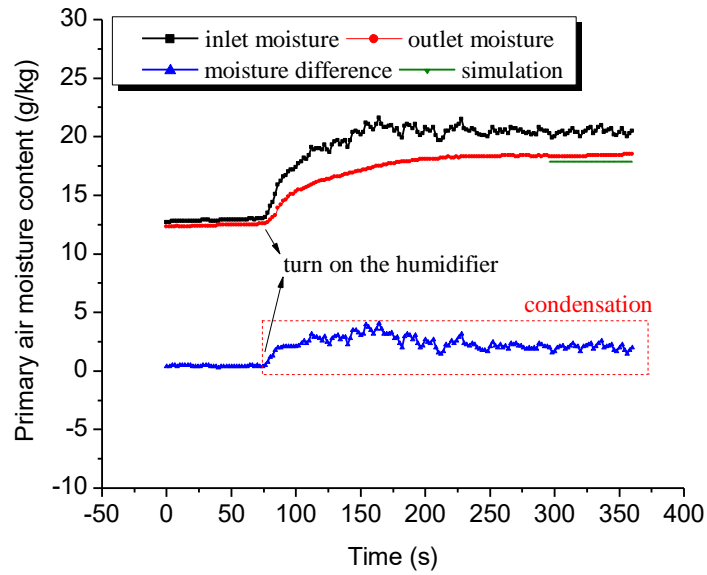
Fig.8 shows the temperature and humidity variation of outlet primary air when the air cooler is switched from dry to wet operating mode under high humidity inlet air condition. Unlike the case in section 5.2.1, condensation occurs in this case as the inlet air humidity is high (RH=76%), results in reduction of outlet air moisture content. The outlet primary air temperature decreases from 26.3°C to 24.4°C as soon as the pump is turned on. Meanwhile, the moisture content of the outlet primary air decreases from 19.4 g/kg to 17.2 g/kg, indicating the latent heat is removed by condensation. The principle can be explained as follows. The plate surface temperature is lowered by the water evaporation under wet operating mode, so that the dew point temperature of high humidity air can be higher than the plate surface temperature, results in condensation and dehumidification. In sum, the transition from dry to wet operating mode under high humidity air condition can bring two benefits: increasing the sensible heat transfer rate and enhancing the latent heat transfer rate.

It can be calculated that the sensible heat transfer rate under dry operating mode in Fig.8 is 290 kW; while it is 472 kW under wet operating mode. In addition, the latent heat transfer rate under wet operating mode is 524 kW. So the total heat transfer rate is greatly improved by 2.4 times when switching the operating mode from dry to wet. The enlargement of total heat transfer rate under high humidity condition is more significant than that of low humidity condition.

5.2.3 Switch from low to high humidity inlet primary air (wet operating mode)



(a) outlet primary air temperature



(b) outlet primary air moisture content

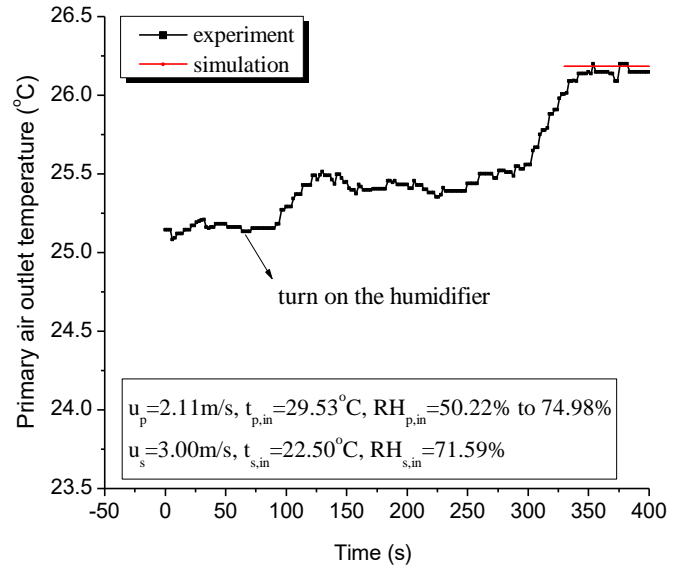
Fig.9 Outlet air condition variation when switching from low to high humidity inlet primary air (wet operating mode)

Fig.9 shows the temperature and humidity variation of outlet primary air when the inlet primary air is switched from low humidity to high humidity under wet operating mode. It can be seen that the outlet primary air temperature increases from 23.0°C to 24.7°C as soon as the humidifier is turned on. During the transition process, the relative humidity of inlet primary air increases from 48.8% to 84.7%. The rise of outlet air temperature shows a decline of sensible heat transfer rate. Meanwhile, there is a significant moisture content difference (3.1 g/kg in average) between the inlet and outlet primary air, which indicates the condensation from primary air. So the latent heat transfer of the air cooler is enhanced by condensation.

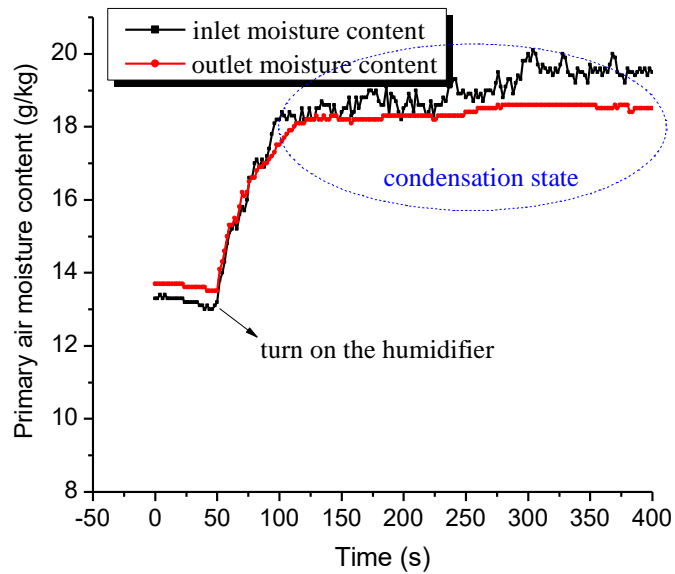
In sum, the transition of IEC operating mode from non-condensation to condensation will reduce the sensible heat transfer rate but improves latent heat transfer rate. It can be explained as follows. The heat released during the condensation process will increase the plate surface temperature, thus the driving force of sensible heat transfer between the plate surface and primary air will be lowered. In Fig.9, the sensible cooling capacity of IEC under non-condensation state is calculated to be 608W; while it is 454W under condensation state. The sensible heat transfer rate is reduced by 25% owing to the condensation. The latent heat transfer rate, however, increases from 0 to 701W, making the total heat transfer rate 1155 kW under condensation state. Thus, the total cooling capacity is enlarged by 90%. It can be deduced that the IEC has a very promising potential for energy recovery in an air-conditioning system in hot and humid regions, because of its advantages in reducing both sensible and latent load.



5.2.4 Switch from low to high humidity inlet primary air (dry operating mode)



(a) outlet primary air temperature



(b) outlet primary air moisture content

Fig.10 Outlet air variation process when switching from low to high humidity inlet primary air (dry operating mode)

Fig.10 shows the temperature and humidity variation of outlet primary air when the inlet primary air is switched from low humidity to high humidity under dry operating mode. Similar with the

pervious case in section 5.2.3, the outlet primary air temperature increases and moisture content decreases because of condensation. The outlet primary air temperature increases by 1.0 °C, results in a reduction of sensible heat transfer rate by 99 kW. The outlet primary air moisture content decreases by 0.7 g/kg, results in an increase of latent heat transfer rate by 247 kW. The total heat transfer rate is improved by 34%. The increase of latent and total heat transfer rate in this case is less significant than the case in section 5.2.3. The reason can be explained as: the plate surface temperature of the air cooler under wet operating mode is lower than that of dry operating mode, so the driving force of latent heat transfer (difference between the saturated moisture content at plate surface temperature and mainstream primary air moisture content) is larger than that of dry operating mode.

### **5.3 Influence of parameters**

The influences of  $t_{p,in}$ ,  $u_{p,in}$ ,  $t_{s,in}$  and  $u_{s,in}$  variation under four operating modes are discussed. Under low humidity condition, the sensible efficiency  $\eta$  and wet-bulb efficiency  $\eta_{wb}$  are used for rating the traditional air cooler and IEC, respectively. Under high humidity condition, the latent efficiency  $\eta_{lat}$  is also used except for  $\eta$  and  $\eta_{wb}$ . Besides, the simulation results by numerical model [43] under each case are given in order to be compared with experiment results.

### 5.3.1 Influence of primary air temperature

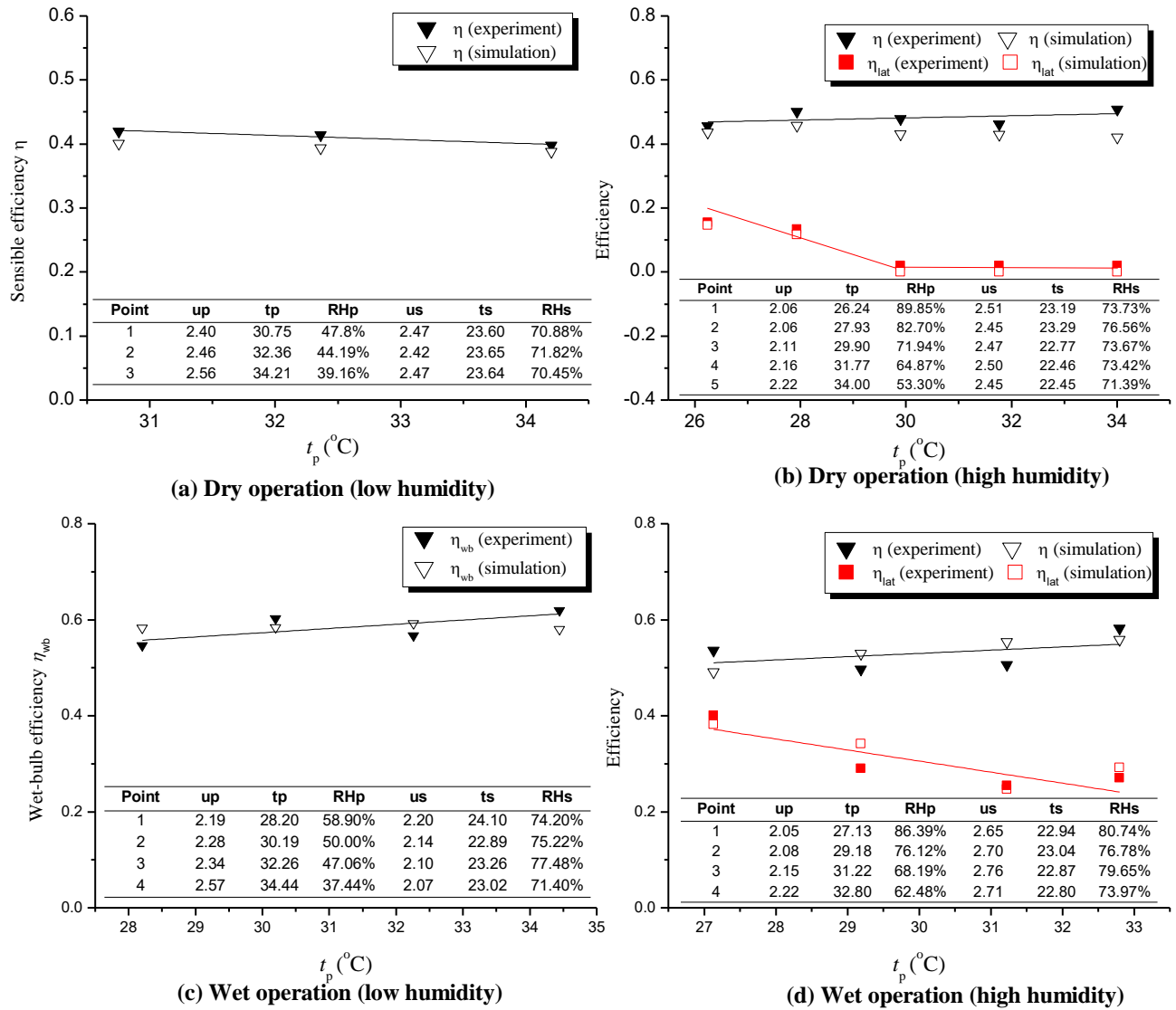


Fig.11 Influence of primary air temperature under four operating modes

Fig.11 presents the influence of primary air temperature under four operating modes. It can be seen that sensible efficiency is not sensitive to  $t_p$  increase under dry operation mode. The sensible efficiency varies in a very small range between 40% ~42% under low humidity condition and 46%~51% under high humidity condition, as shown in Fig.11(a) and Fig.11(b). The latent

efficiency, however, decreases from 16% to 0 with  $t_{p,in}$  increases from 26°C to 34°C under high humidity condition. The decrease of latent efficiency is because the condensation is weakened as the plate surface temperature increases.

The influence of  $t_p$  has larger impact on the air cooler under wet operating mode (IEC). The wet-bulb efficiency increases from 55% to 62% under low air humidity condition and increases from 54% to 58% under high air humidity condition, as shown in Fig.11(c) and Fig.11(d). The wet-bulb efficiency increase rate under high air humidity condition is less significant than that of low air humidity condition. It is because the condensation increases the plate surface temperature by releasing latent heat and brings negative effect on sensible heat transfer. Besides, the increase of  $t_{p,in}$  has significant negative effect on the latent heat transfer by rising the plate surface temperature. As shown in Fig.11(d), the latent efficiency decreases from 40% to 27% when  $t_{p,in}$  increases from 27°C to 33°C.

### 5.3.2 Influence of primary air velocity

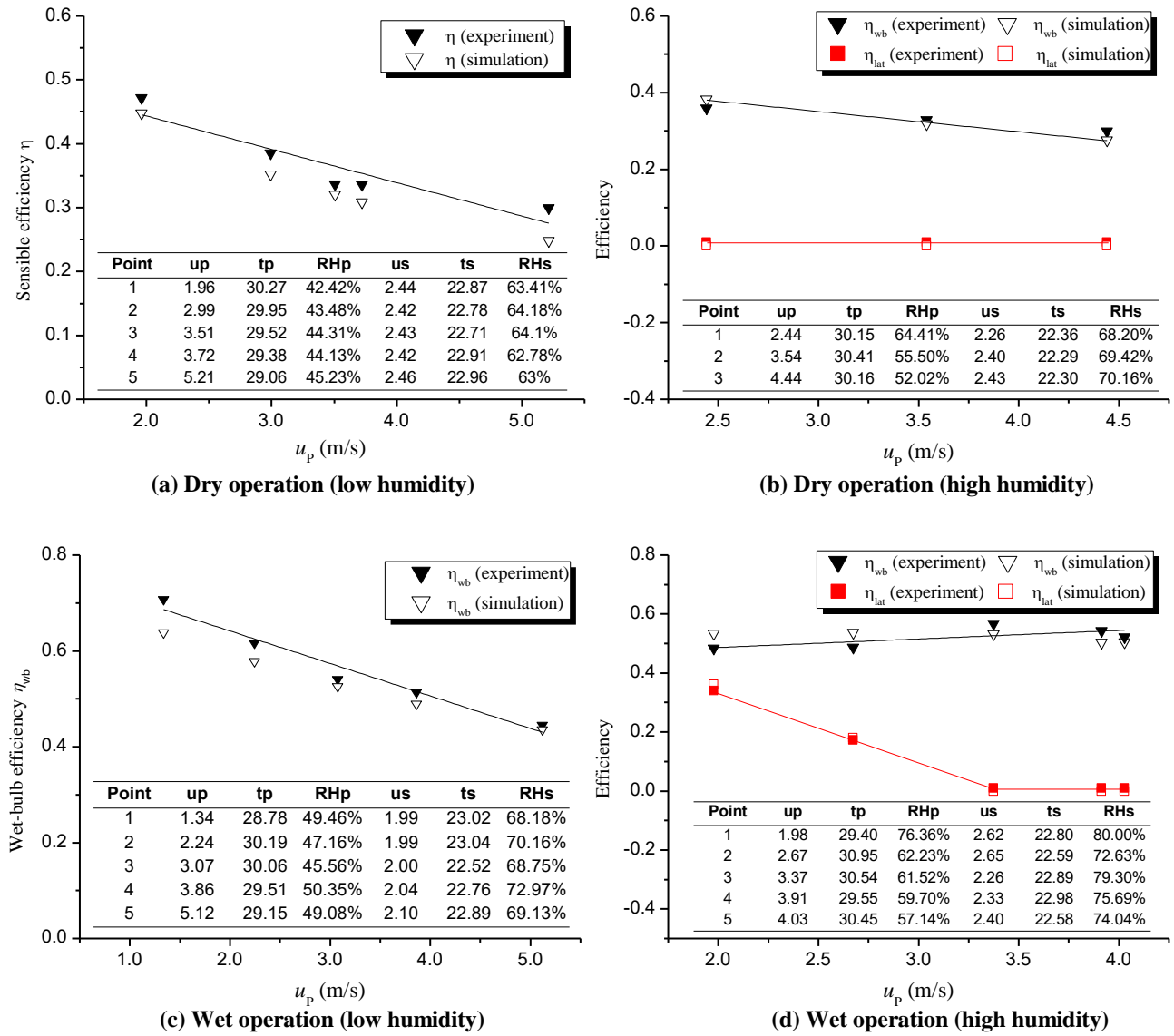


Fig.12 Influence of primary air velocity under four operating modes

Fig.12 presents the influence of primary air velocity under four operating modes. It can be seen from Fig.12(a) that the sensible efficiency  $\eta$  decreases from 47% to 30% when  $u_p$  increases from 2.0 m/s to 5.2 m/s under dry operating mode with low humidity inlet air. The same conclusion

can be drawn to the wet operating mode (IEC). The  $\eta_{wb}$  decreases from 64% to 44% when  $u_p$  increases from 1.3 m/s to 5.1 m/s as shown in Fig.12(c).

The air cooler operates under high humidity condition can be different from that of low humidity condition because the condensation is involved. The condensation from primary air results in latent heat transfer, and influences the sensible heat transfer as well. In Fig.12(d), it can be seen that the latent efficiency  $\eta_{lat}$  decreases from 34% to 0 when  $u_p$  increases from 2.0 m/s to 4.0 m/s, indicating the IEC operation state switches from condensation to non-condensation. Meanwhile,  $\eta_{wb}$  increase a little from 49% to 52%. The increase of  $u_p$  affects  $\eta$  and  $\eta_{wb}$  from two aspects. On one hand,  $\eta$  and  $\eta_{wb}$  decreases as the increase of cooled media, on the other hand, the latent efficiency could decline to zero, switching the operation state from condensation to non-condensation. This improves the sensible efficiency by eliminating condensation. The comprehensive effects decide the variation of  $\eta_{wb}$ .

### 5.3.3 Influence of secondary air temperature

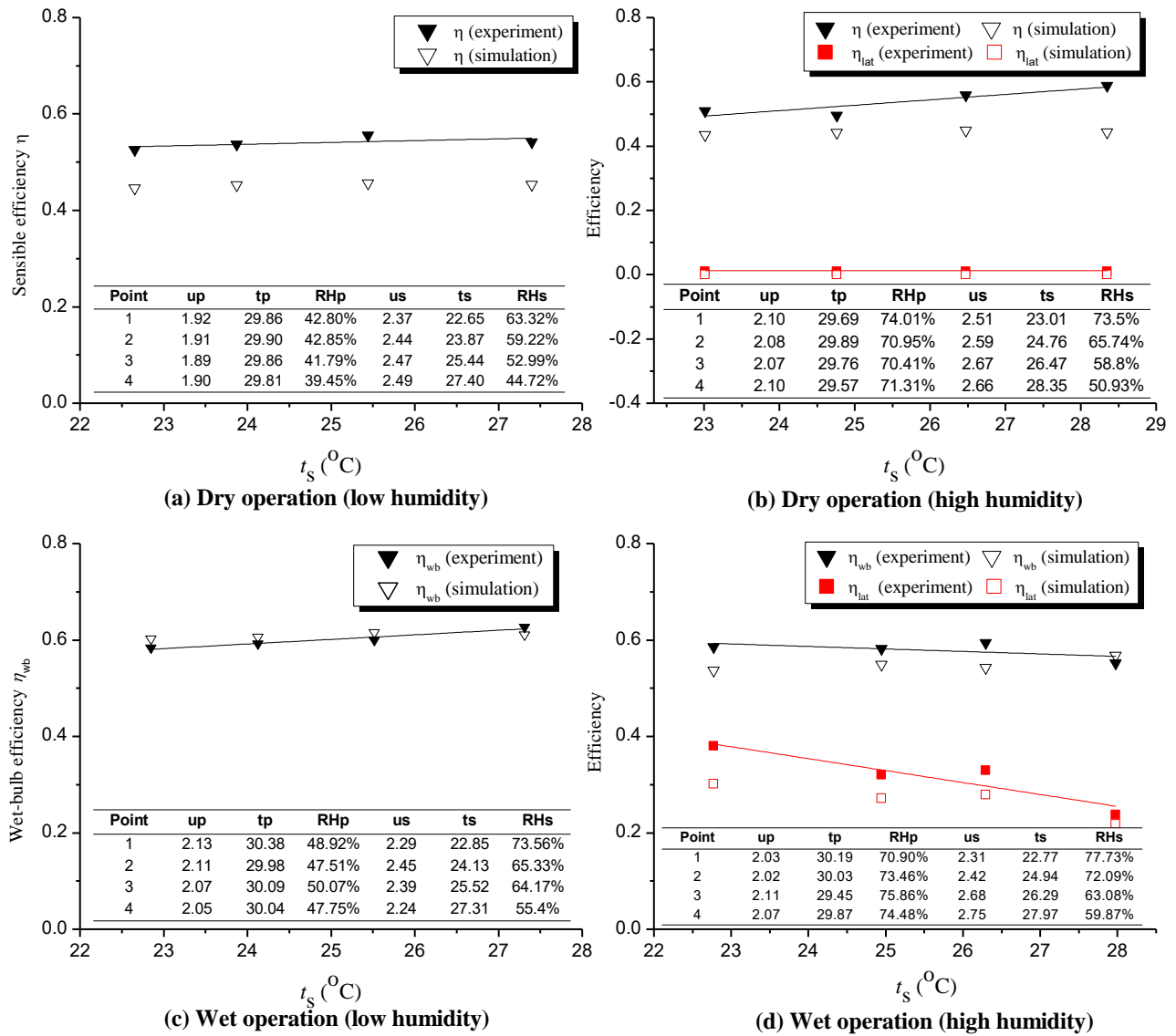


Fig.13 Influence of secondary air temperature under four operating modes

Fig.13 presents the influence of secondary air temperature under four operating modes. It can be seen from Fig.13(a) that the sensible efficiency  $\eta$  increases a little from 52.7% to 54.2% with  $t_s$  increases from 22.6°C to 27.4°C under dry operation mode. The same conclusion can be drawn to the wet operating mode (IEC). The  $\eta_{wb}$  increases from 58% to 63% when  $t_s$  increases from

22.8°C to 27.3°C as shown in Fig.13(c). So the thermal efficiency of IEC is more sensitive to the change of  $t_s$  compared with that of traditional air cooler.

Under wet operating mode with high inlet air humidity (Fig.13(d)), it can be seen that  $\eta_{\text{lat}}$  decreases significantly from 38% to 24% with  $t_s$  increases from 22.8°C to 28°C, while  $\eta_{\text{sen}}$  fluctuates a little. The decline of  $\eta_{\text{lat}}$  can be attributed to the rise of plate surface temperature as  $t_s$  increases. In addition, it is much easier to condense in IEC compared with traditional air cooler by comparing Fig.13(c) and Fig.13(d). In Fig.13(c), no condensation occurs even when  $\text{RH}_p$  exceeds 70%. In Fig.13(d), however, condensation exists under all air conditions.



### 5.3.4 Influence of secondary air velocity

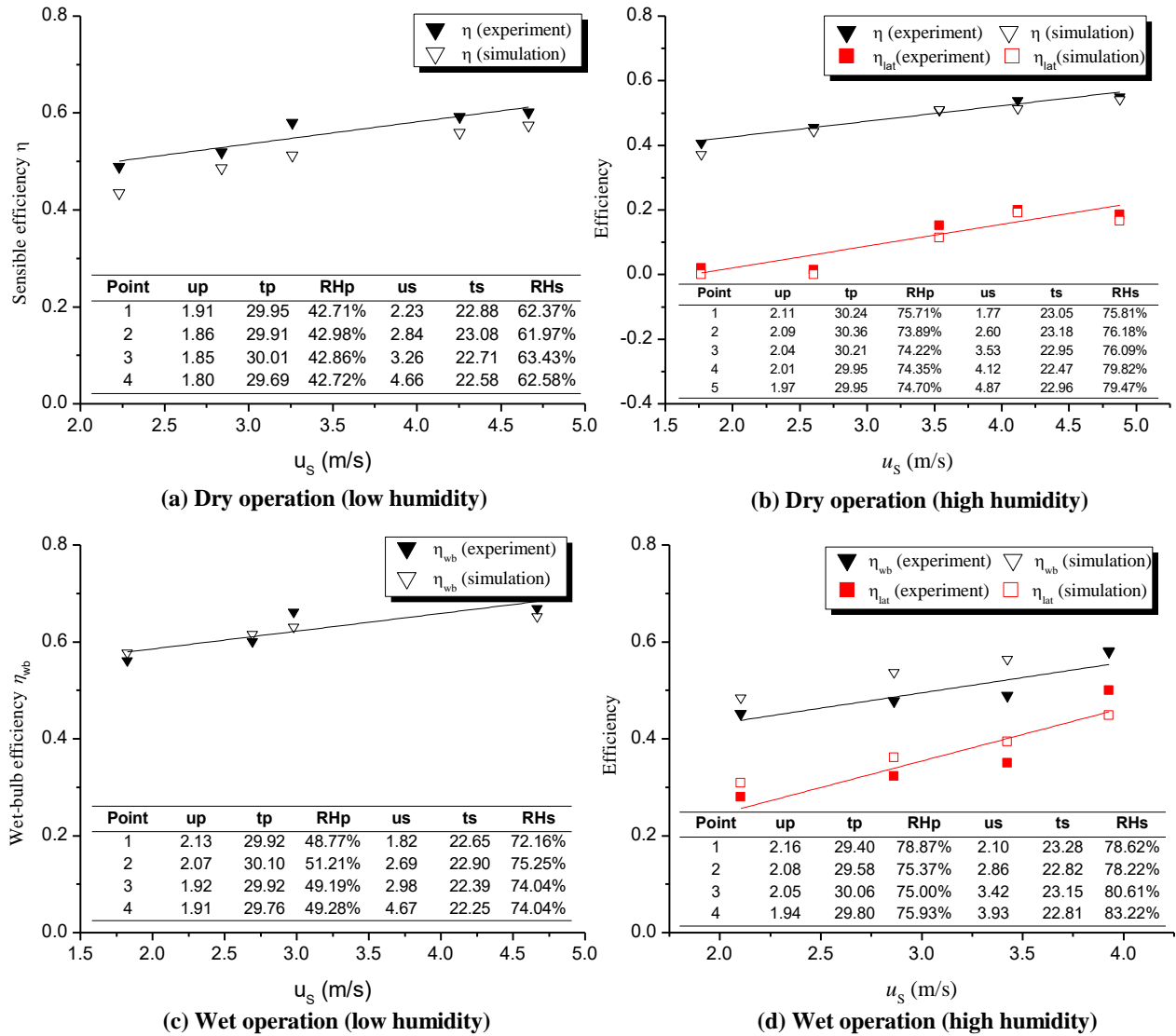


Fig.14 Influence of secondary air velocity under four operating modes

Fig.14 presents the influence of secondary air velocity under four operating modes. It can be seen from Fig.14(a) that the sensible efficiency  $\eta$  increases significantly from 49% to 60% with  $u_s$  increases from 2.2 m/s to 4.7 m/s under dry operating mode with low humidity inlet air. The

same conclusion can be drawn to the wet operating mode (IEC) with low humidity inlet air. The  $\eta_{wb}$  increases from 56% to 67% when  $u_s$  increases from 1.8 m/s to 4.7 m/s as shown in Fig.14(c).

Under high humidity conditions, both sensible efficiency  $\eta$  and latent efficiency  $\eta_{lat}$  of traditional air cooler increase with the increase of  $u_s$ . The  $\eta$  improves from 41% to 55% and  $\eta_{lat}$  increase from 0 to 19% as shown in Fig,14(b). So  $u_s$  has a great impact on the air cooler thermal performance and can even change its operation state from non-condensation to condensation. Similarly, both  $\eta_{wb}$  and  $\eta_{lat}$  for IEC improve dramatically from 45% to 58% and 28% to 50%, respectively, with  $u_s$  increases from 2.1 m/s to 3.9 m/s (Fig,14(d)). The increase of  $\eta_{lat}$  is more significant than that of  $\eta_{wb}$ . In sum, increasing  $u_s$  is an effective way to improve the sensible and latent cooling capacities for both IEC and traditional air cooler.

## 5.4 Cooling capacity analysis

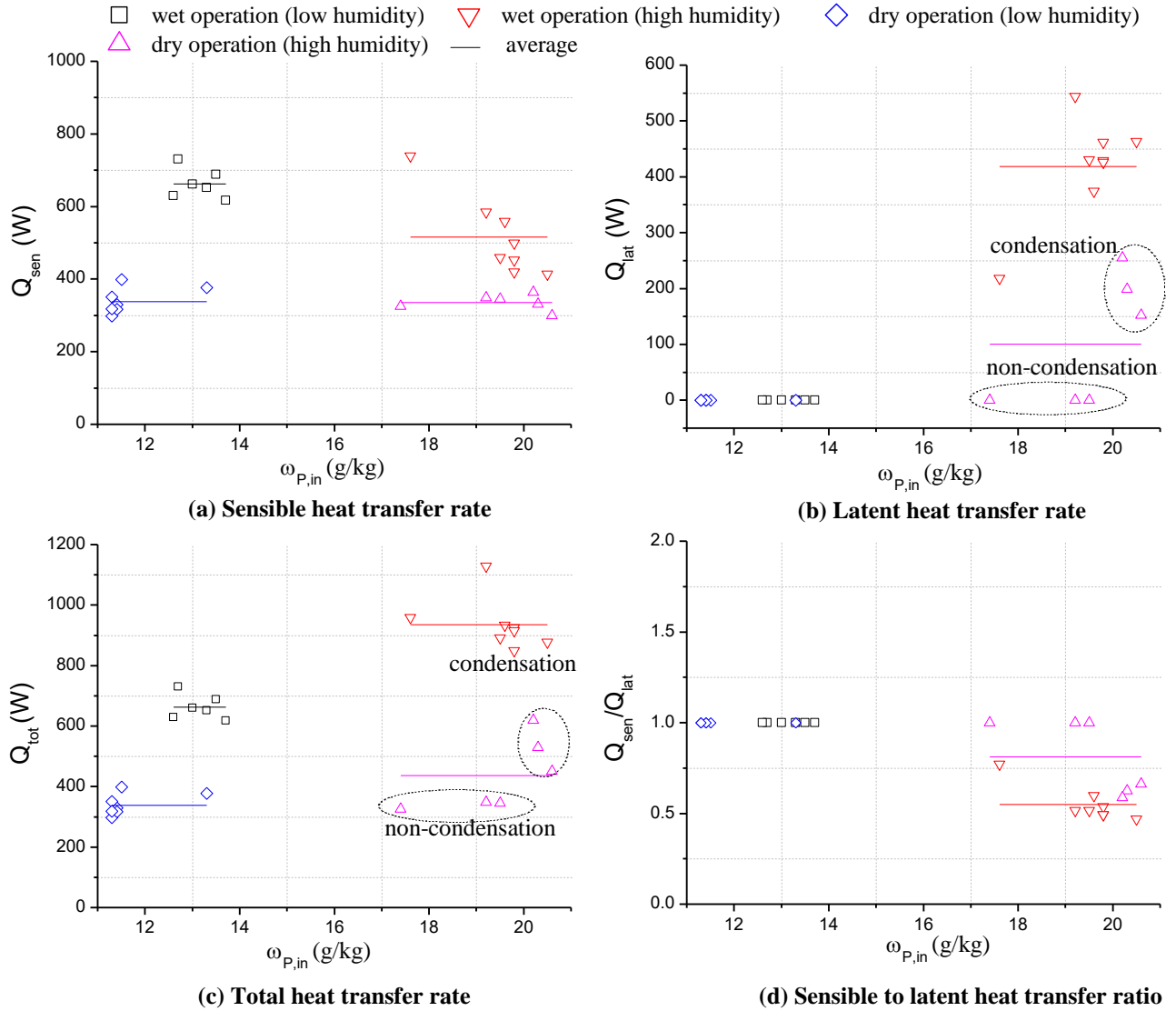


Fig.15 Comparison of cooling capacities under four operation modes

Different cooling capacities, including  $Q_{sen}$ ,  $Q_{lat}$  and  $Q_{tot}$ , are compared among four operating modes under the same conditions as shown in Fig.15 ( $t_p \approx 30$  °C,  $u_p \approx 2$  m/s,  $t_s \approx 23$  °C,  $RH_s \approx 70\%$ ,  $u_s \approx 2.5$  m/s). It can be seen that the ranking for  $Q_{sen}$  is: wet operation (low humidity) > wet operation (high humidity) > dry operation (low humidity) > dry operation (high humidity); the

ranking for  $Q_{lat}$  is: wet operation (high humidity) > dry operation (high humidity) > wet operation (low humidity) = dry operation (low humidity) and the ranking for  $Q_{tot}$  is: wet operation (high humidity) > wet operation (low humidity) > dry operation (high humidity) > dry operation (low humidity). So the IEC performs much better than the traditional air cooler no matter under low humidity or high humidity regions. The  $Q_{sen}$  of IEC under low humidity condition is 96% larger than that of the traditional air cooler. The  $Q_{lat}$  of IEC is 3.1 times larger than that of traditional air cooler. The  $Q_{tot}$  of IEC under high humidity condition is 176% larger than that of traditional air cooler under low humidity condition. Besides, as shown in Fig.15(d),  $Q_{sen}/Q_{lat}$  of IEC under high humidity condition is 0.62, so  $Q_{lat}$  accounts for a large proportion of  $Q_{tot}$  under condensation state.

### 5.5 Energy consumption and COP

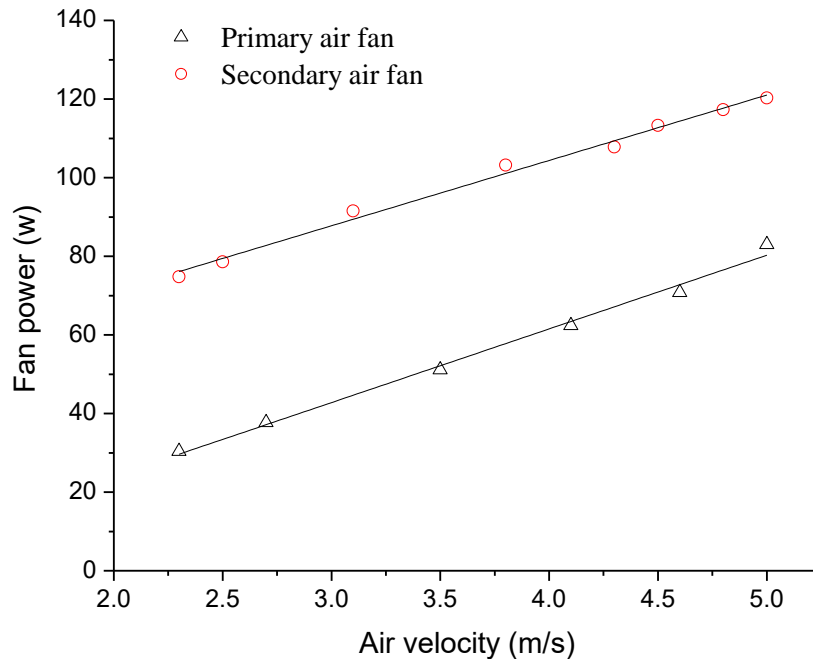


Fig.16 Fan power consumption measured under different air velocity

Fig.16 shows the fan power consumption measured by the power meter under different air velocity. The nominal power of the primary air fan and secondary air fan are 95W and 120W, respectively. The supply air flow rate is adjusted by the fan speed controller. It can be seen that fan power increases linearly with air velocity increases. The measured fan power consumptions are used for COP calculation thereafter.

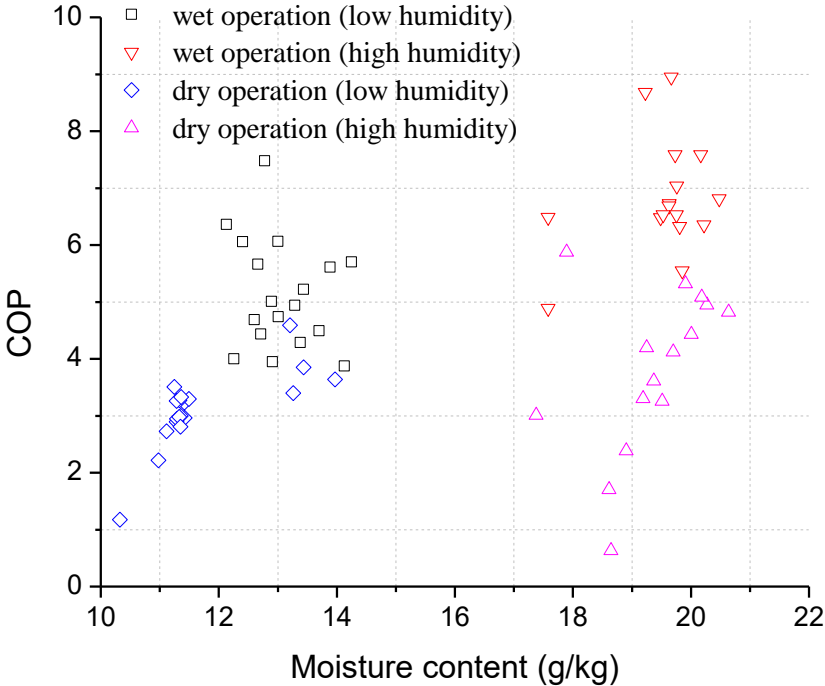


Fig.17 COP of air cooler under four operating modes

Fig.17 shows the COP of air cooler under four operating modes. It can be seen that COP varies in a wide range because the cooling capacity of the air cooler depends largely on the ambient air conditions. The average COP ranking among the four operating modes is: wet operation (high humidity) > wet operation (low humidity) > dry operation (high humidity) > dry operation (low humidity). The highest COP can reach up to 9.0 under wet operating mode. However, the maximum COP of the air cooler under dry operating mode can only reach 6.0. Thus, it is highly

efficient to apply IEC in hot and humid regions for energy recovery in an air-conditioning system.

## **6. Conclusion**

This paper presents an experimental study of plate type air cooler performance under four operating modes. The air cooler works as a traditional cooler under dry operating mode and works as an indirect evaporative cooler (IEC) under wet operating mode. The cooler dynamic performances during different operating mode transition were investigated. The steady performances under different parameter influence were also comparatively studied. The highlighted results are summarized as follows:

1. By switching the air cooler from dry to wet operating mode, the outlet primary air temperature could be significantly reduced ( $2^{\circ}\text{C}\sim 3^{\circ}\text{C}$  in the studied case). Under high humidity inlet air condition, condensation or dehumidification ( $2.2\text{ g/kg}$  in the studied case) was observed when switching operating mode from dry to wet. Thus, not only sensible but also latent cooling load could be reduced by IEC when it is applied in hot and humid regions for energy recovery.
2. By switching the air cooler from low to high humidity operating mode, condensation could be observed and the outlet primary air temperature increases accordingly, which means that the sensible heat transfer decreases while latent heat transfer increases. The dehumidification by IEC ( $3.1\text{ g/kg}$  in the studied case) is much more obvious than that of traditional air cooler ( $0.7\text{ g/kg}$  in the studied case).

3. The  $\eta$  and  $\eta_{wb}$  are improved by increasing  $t_{p,in}$ , and  $u_s$ , and decreasing  $u_p$  and  $t_{s,in}$ , of which decreasing  $u_p$  and increasing  $u_s$  are most effective. The  $\eta_{lat}$  can be improved by decreasing  $t_{p,in}$ ,  $u_p$  and  $t_{s,in}$ , and increasing  $u_s$ . The thermal efficiency of IEC is more sensitive to the parameters variation compared with traditional air cooler.
4. The sensible, latent and total cooling capacities ( $Q_{sen}$ ,  $Q_{lat}$  and  $Q_{tot}$ ) were compared among four operating modes under the same air conditions and cooler configuration. The IEC performed much better than the traditional air cooler under both low and high humidity conditions. The  $Q_{tot}$  of IEC under high humidity condition is 176% larger than that of traditional air cooler under low humidity condition.
5. The COP of air cooler under four operating modes were compared. The COP varies in a wide range under different operating mode. The highest COP (9.0) was achieved by IEC under high air humidity. The COP of the air cooler with high humidity inlet air is higher than that of low humidity inlet air, so it is highly efficient for operating IEC in hot and humid regions for energy recovery in an air-conditioning system

### **Acknowledgement**

This research is financially supported by the Research Institute of Sustainable Urban Development of The Hong Kong Polytechnic University and the Housing Authority of the Hong Kong SAR Government with account No. K-ZJK1.

### **References**

- [1] Pérez-Lombard, L., Ortiz, J., & Pout, C. (2008). A review on buildings energy consumption information. *Energy and buildings*, 40(3), 394-398.
- [2] Barbhuiya, S., & Barbhuiya, S. (2013). Thermal comfort and energy consumption in a UK educational building. *Building and Environment*, 68, 1-11.
- [3] Hong Kong Energy End-Use Data, Electrical and Mechanical Services Department of Hong Kong Special Administrative Region, 2015.  
[http://www.emsd.gov.hk/filemanager/en/content\\_762/HKKEUD2015.pdf](http://www.emsd.gov.hk/filemanager/en/content_762/HKKEUD2015.pdf)
- [4] ASHRAE handbook, 2008. Heating, Ventilating, and Air-Conditioning Systems and Equipment (I-P Edition), American Society of Heating, Refrigerating and Air-Conditioning Engineers, Inc., 2008.
- [5] Hewitt, G. F. (2008). Heat exchanger design handbook (Vol. 98). Begell House.
- [6] Barrow, H., Mistry, J., & Clayton, D. (1986). Numerical and Exact Mathematical Analyses of Two Dimensional Rectangular Composite Fins. In Proc. 8th International Heat Transfer Conference, San Francisco (Vol. 2, pp. 367-372).
- [7] Huang, L. J., & Shah, R. K. (1992). Assessment of calculation methods for efficiency of straight fins of rectangular profile. *International journal of heat and fluid flow*, 13(3), 282-293.
- [8] An, C. S., & Choi, D. H. (2012). Analysis of heat-transfer performance of cross-flow fin-tube heat exchangers under dry and wet conditions. *International Journal of Heat and Mass Transfer*, 55(5), 1496-1504.
- [9] Fernández-Seara, J., Diz, R., Uhía, F. J., Dopazo, A., & Ferro, J. M. (2011). Experimental analysis of an air-to-air heat recovery unit for balanced ventilation systems in residential buildings. *Energy conversion and management*, 52(1), 635-640.



- [10] Gendebien, S., Bertagnolio, S., & Lemort, V. (2013). Investigation on a ventilation heat recovery exchanger: Modeling and experimental validation in dry and partially wet conditions. *Energy and buildings*, 62, 176-189.
- [11] Liu, Z., Allen, W., & Modera, M. (2013). Simplified thermal modeling of indirect evaporative heat exchangers. *HVAC&R Research*, 19(3), 257-267.
- [12] Porumb, B., Ungureșan, P., Tutunaru, L. F., Șerban, A., & Bălan, M. (2016). A Review of Indirect Evaporative Cooling Operating Conditions and Performances. *Energy Procedia*, 85, 452-460.
- [13] Porumb, B., Ungureșan, P., Tutunaru, L. F., Șerban, A., & Bălan, M. (2016). A Review of Indirect Evaporative Cooling Technology. *Energy Procedia*, 85, 461-471.
- [14] Krüger, E., González Cruz, E., & Givoni, B. (2010). Effectiveness of indirect evaporative cooling and thermal mass in a hot arid climate. *Building and Environment*, 45(6), 1422-1433.
- [15] Jaber, S., & Ajib, S. (2011). Evaporative cooling as an efficient system in Mediterranean region. *Applied Thermal Engineering*, 31(14), 2590-2596.
- [16] Bajwa, M., Aksugur, E., & Al-Otaibi, G. (1993). The potential of the evaporative cooling techniques in the gulf region of the Kingdom of Saudi Arabia. *Renewable energy*, 3(1), 15-29.
- [17] Cruz, E. G., & Krüger, E. (2015). Evaluating the potential of an indirect evaporative passive cooling system for Brazilian dwellings. *Building and Environment*, 87, 265-273.
- [18] Zhao, X., Yang, S., Duan, Z., & Riffat, S. B. (2009). Feasibility study of a novel dew point air conditioning system for China building application. *Building and Environment*, 44(9), 1990-1999.

- [19] Chen PL, Qin H, Huang YJ, Wu H, Blumstein C. The energy-saving potential of precooling incoming outdoor air by indirect evaporative cooling. *ASHRAE Trans* 1993;99(Pt 1).
- [20] Delfani, S., Esmaeelian, J., Pasharshahi, H., & Karami, M. (2010). Energy saving potential of an indirect evaporative cooler as a pre-cooling unit for mechanical cooling systems in Iran. *Energy and Buildings*, 42(11), 2169-2176.
- [21] Jain, V., Mullick, S. C., & Kandpal, T. C. (2013). A financial feasibility evaluation of using evaporative cooling with air-conditioning (in hybrid mode) in commercial buildings in India. *Energy for Sustainable Development*, 17(1), 47-53.
- [22] Cianfrini, C., Corcione, M., Habib, E., & Quintino, A. (2014). Energy performance of air-conditioning systems using an indirect evaporative cooling combined with a cooling/reheating treatment. *Energy and Buildings*, 69, 490-497.
- [23] Hasan, A. (2012). Going below the wet-bulb temperature by indirect evaporative cooling: Analysis using a modified  $\varepsilon$ -NTU method. *Applied Energy*, 89(1), 237-245.
- [24] Ren, C., & Yang, H. (2006). An analytical model for the heat and mass transfer processes in indirect evaporative cooling with parallel/counter flow configurations. *International journal of heat and mass transfer*, 49(3), 617-627.
- [25] Hettiarachchi, H. D., Golubovic, M., & Worek, W. M. (2007). The effect of longitudinal heat conduction in cross flow indirect evaporative air coolers. *Applied Thermal Engineering*, 27(11), 1841-1848.
- [26] Yang, H., Ren, C., & Cui, P. (2006). Study on performance correlations of an indirect evaporative cooler with condensation from primary airflow. *HVAC&R Research*, 12(3), 519-532.

- [27] Chen, Y., Luo, Y., & Yang, H. (2015). A simplified analytical model for indirect evaporative cooling considering condensation from fresh air: Development and application. *Energy and Buildings*, 108, 387-400.
- [28] Riangvilaikul, B., & Kumar, S. (2010). Numerical study of a novel dew point evaporative cooling system. *Energy and Buildings*, 42(11), 2241-2250.
- [29] Tulsidasani, T. R., Sawhney, R. L., Singh, S. P., & Sodha, M. S. (1997). Recent research on an indirect evaporative cooler (IEC) part 1: optimization of the COP. *International journal of energy research*, 21(12), 1099-1108.
- [30] Qiu G. A Novel Evaporative/Desiccant Cooling System [PhD]. The University of Nottingham; 2007.
- [31] Velasco Gómez, E., Tejero González, A., & Rey Martínez, F. J. (2012). Experimental characterization of an indirect evaporative cooling prototype in two operating modes. *Applied Energy*, 97, 340-346.
- [32] Jain, D. (2007). Development and testing of two-stage evaporative cooler. *Building and Environment*, 42(7), 2549-2554.
- [33] Kulkarni, R. K., & Rajput, S. P. S. (2011). Performance evaluation of two stage indirect/direct evaporative cooler with alternative shapes and cooling media in direct stage. *International Journal of Applied Engineering Research*, Dindigul, 1(4), 800-812.
- [34] El-Dessouky, H., Ettouney, H., & Al-Zeefari, A. (2004). Performance analysis of two-stage evaporative coolers. *Chemical Engineering Journal*, 102(3), 255-266.

- [35] Heidarinejad, G., Bozorgmehr, M., Delfani, S., & Esmaeelian, J. (2009). Experimental investigation of two-stage indirect/direct evaporative cooling system in various climatic conditions. *Building and Environment*, 44(10), 2073-2079.
- [36] Jain, D. (2007). Development and testing of two-stage evaporative cooler. *Building and Environment*, 42(7), 2549-2554.
- [37] Duan, Z., Zhan, C., Zhao, X., & Dong, X. (2016). Experimental study of a counter-flow regenerative evaporative cooler. *Building and Environment*, 104, 47-58.
- [38] Elberling L. Laboratory Evaluation of the Coolerado Cooler – Indirect Evaporative Cooling Unit. Pacific Gas and Electric Company, 2006.
- [39] Riangvilaikul, B., & Kumar, S. (2010). An experimental study of a novel dew point evaporative cooling system. *Energy and Buildings*, 42(5), 637-644.
- [40] Zhan, C., Duan, Z., Zhao, X., Smith, S., Jin, H., & Riffat, S. (2011). Comparative study of the performance of the M-cycle counter-flow and cross-flow heat exchangers for indirect evaporative cooling—paving the path toward sustainable cooling of buildings. *Energy*, 36(12), 6790-6805.
- [41] Duan, Z. (2011) Investigation of a Novel Dew Point Indirect Evaporative Air Conditioning System for Buildings [Ph.D. Thesis]. Nottingham University of Nottingham.
- [42] H.W. Coleman, W.G. Steele, *Experimentation, Validation, and Uncertainty Analysis for Engineers*, third ed., A John Wiley & Sons, Inc., 2009.
- [43] Chen, Y., Yang, H., & Luo, Y. (2016). Indirect evaporative cooler considering condensation from primary air: Model development and parameter analysis. *Building and Environment*, 95, 330-345.